

Cite this article as:
Sakai NS, Taylor SA, Chouhan MD. Obesity, metabolic disease and the pancreas—Quantitative imaging of pancreatic fat. *Br J Radiol* 2018;
91: 20180267.

THE ROLE OF IMAGING IN OBESITY SPECIAL FEATURE: REVIEW ARTICLE

Obesity, metabolic disease and the pancreas— Quantitative imaging of pancreatic fat

NAOMI S SAKAI, MRCS, MA, STUART A TAYLOR, MRCP, FRCR, MD and MANIL D CHOUHAN, MRCS, FRCR, PhD

UCL Centre for Medical Imaging, Division of Medicine, University College London, London, UK

Address correspondence to: Dr Manil D Chouhan
E-mail: manil.chouhan@gmail.com

ABSTRACT

The association between pancreatic fat, obesity and metabolic disease is well-documented, and although a potentially exciting target for novel therapies, remains poorly understood. Non-invasive quantitative imaging-derived biomarkers can provide insights into pathophysiology and potentially provide robust trial endpoints for development of new treatments. In this review, we provide an overview of the pathophysiology of non-alcoholic fatty pancreas disease and associations with metabolic factors, obesity and diabetes. We then explore approaches to pancreatic fat quantification using ultrasound, CT and MRI, reviewing the strengths, limitations and current published evidence in the assessment of pancreatic fat. Finally, we explore the broader challenges of pancreatic fat quantification as we move toward translating these methods into the clinical setting.

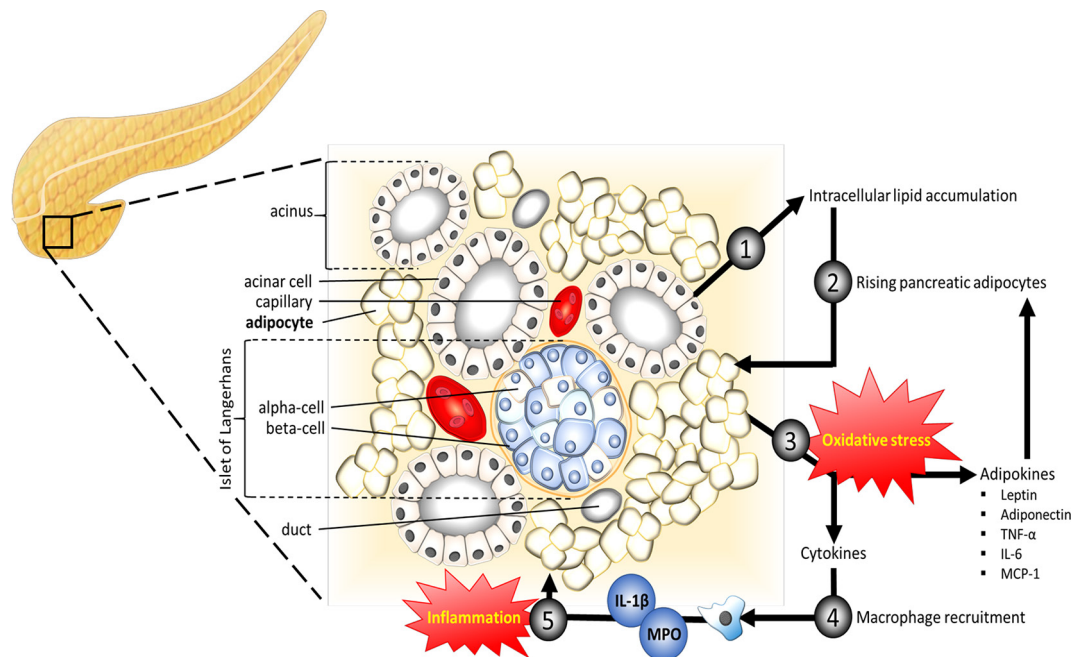
FAT AND THE PANCREAS

Obesity, as defined by Body Mass Index (BMI) exceeding 30 kg/m², is a major global economic and public health challenge, with the UK prevalence increasing from 15 to 27% since 1993¹ and expected to reach 35% by 2030.² Obesity is a known cause of ectopic fat accumulation in organs including the pancreas.³ Fatty infiltration of the pancreas (pancreatic steatosis) in obesity was first described in 1933⁴ and has since been linked to pancreatitis,⁵ the metabolic syndrome and Type 2 diabetes mellitus (T2DM).⁶ The pathophysiology of pancreatic steatosis and its sequelae are less well-understood than in the liver, and remain an area of ongoing research. Pancreatic steatosis is linked to a number of congenital and acquired factors including cystic fibrosis, age, alcohol excess, viral infections and drugs,⁷ but the association with metabolic factors (obesity and T2DM) have driven renewed interest. Research has been hampered by the lack of standardised nomenclature, with the use of various terms, for example, pancreatic steatosis, fatty pancreas, fatty infiltration and pancreatic lipomatosis. Recently, however, the term non-alcoholic fatty pancreas disease (NAFPD) has gained acceptance in describing pancreatic steatosis in association with obesity and the metabolic syndrome.⁸ Whilst a recent meta-analysis quantified normal mean pancreatic fat at 4.5 ± 0.9% (based on pooled data across multiple MR methods and imaging

modalities),⁹ progress has also been slowed by the lack of a precise consensus threshold on the upper limit of normal pancreatic fat content.

Histologically, NAFPD is a heterogenous process, characterised by increased intracellular lipid accumulation and adipocyte infiltration in the pancreatic tissue. Islet cells themselves are thought to be resistant to fatty infiltration but it has been suggested that the overall process is similar to that seen in the liver [where non-alcoholic fatty liver disease (NAFLD) progresses to non-alcoholic steatohepatitis (NASH)], with NAFPD progressing to non-alcoholic fatty steatopancreatitis (NASP) (Figure 1). Under conditions of oxidative stress, fat-derived cytokines are released and result in localised inflammation and organ dysfunction. In addition, adipose itself has endocrine capabilities, producing adipocytokines, including leptin, adiponectin, tumour necrosis factor alpha (TNF-α), interleukin-6 (IL-6) and monocyte chemoattractant protein-1 (MCP-1).^{10–12} Recruited macrophages in turn produce IL-1β and myeloperoxidase, which further exacerbate the inflammatory process. This has led to the hypothesis that NAFPD may increase the risk of developing pancreatitis (and exacerbate its severity),⁸ pancreatic cancer,¹³ beta-cell dysfunction and the development of T2DM.

Figure 1. Pathophysiological mechanisms for non-alcoholic fatty pancreas disease. Intracellular accumulation of lipid¹ is thought to precede the rise in pancreatic tissue adipocytes.² Subsequent oxidative stress leads to the release of adipokines and cytokines⁴ which trigger an inflammatory response⁵ that is ultimately thought to drive beta-cell dysfunction leading to Type 2 diabetes mellitus. MPO, myeloperoxidase; TNF-alpha, tumour necrosis factor-alpha.



Metabolic factors, Type 2 Diabetes Mellitus and NAFPD

The metabolic syndrome is a group of risk factors for cardiovascular disease, T2DM and stroke, which includes obesity, dyslipidaemia, hypertension and raised fasting blood glucose. NAFPD and its relation to age, BMI, atherosclerosis and diabetes was first described in post-mortem studies.¹⁴ Current data suggest that fat distribution is a better marker of metabolic risk than obesity itself¹⁵; this has resulted in great interest in the pancreas as a site of ectopic fat deposition and its role in insulin resistance. More recent research has demonstrated an association between NASH and NAFPD^{6,16,17} and identified a two-fold increase in the risk of metabolic syndrome⁹ in patients with NAFPD.

Ectopic fat accumulation in skeletal muscle and liver is linked to insulin resistance and pancreatic Islet of Langerhans beta-cell dysfunction.^{18–20} Insulin resistance coupled with progressive beta-cell dysfunction is a hallmark of T2DM. The correlation between patients with NASH and NAFPD,²¹ has also driven interest in lipid accumulation in the pancreas as a cause of impaired beta-cell insulin secretion.⁸ The effect of pancreatic fat on insulin resistance and pancreatic beta-cell dysfunction has been investigated in animal and human studies.^{20,22} Pancreatic fat content in humans is associated with BMI, insulin resistance and the metabolic syndrome.^{6,16} It is proposed that there is a combined destructive effect of increased free fatty acids and NAFPD on pancreatic beta- and islet cell function which leads to hyperglycaemia. However, the evidence as to whether fat accumulation in the pancreas causes beta-cell dysfunction has been inconsistent, particularly in the absence of intra-islet cell lipid accumulation.²³ Whilst some studies have shown that

beta-cell function is negatively associated with pancreatic fat content in non-diabetic subjects²⁰ or those with pre-diabetes²⁴ others have suggested no relationship.²⁵ The association between NAFPD and beta-cell dysfunction is thought to be more complex with factors in addition to pancreatic fat being important once diabetes occurs.²⁶ Interestingly, there is a positive correlation between the duration of T2DM and the pancreatic fat content. In addition to fat content, pancreatic volume is believed to influence the risk of diabetes. Individuals with a large pancreatic volume are thought to have a more sizeable reservoir of beta-cells and greater capacity to withstand the various factors that contribute to the development of diabetes. T2DM is thus associated with a smaller pancreatic volume and greater pancreatic fat content relative to normoglycaemic patients without T2DM.²⁷

Quantitative methods for imaging the pancreas

The deep retroperitoneal location of the pancreas means that there are challenges to studying it non-invasively. This, coupled with its variable shape, often ill-defined boundaries, heterogeneous fat distribution²⁸ and upper abdominal location (with susceptibility to motion artefact), mean that quantitative assessment of pancreatic volume and fat content is challenging across all imaging modalities.

Ultrasound

The pancreas can be assessed using transabdominal or endoscopic ultrasound. The pancreas can usually only be partially visualised with transabdominal ultrasound because of overlying stomach/small intestine gas. Endoscopic ultrasound allows the transducer to be placed in close proximity to the pancreas and therefore has the potential to provide more detailed images of the

whole organ but has the major disadvantage of being invasive. Studies have compared the echotexture of the pancreas to the kidney,^{6,21,29–33} liver³³ or spleen,¹⁶ with the presence of increased pancreatic echogenicity indicative of fatty infiltration. Trans-abdominal ultrasound is a relatively quick and relatively cheap method of imaging the pancreas, is well-tolerated and does not involve ionising radiation. However, it is operator dependent (reported mean interobserver agreement for ultrasound diagnosis of fatty pancreas as low as 72%)²¹ and the pancreas cannot always be visualised (up to 14.5% of all cases),³¹ particularly in obese patients. Crucially, the echotexture of the liver or kidney which the pancreas is compared with may be abnormal and as such ultrasound echogenicity or echogenicity ratios do not provide reliable quantitative information.

Ultrasound elastography

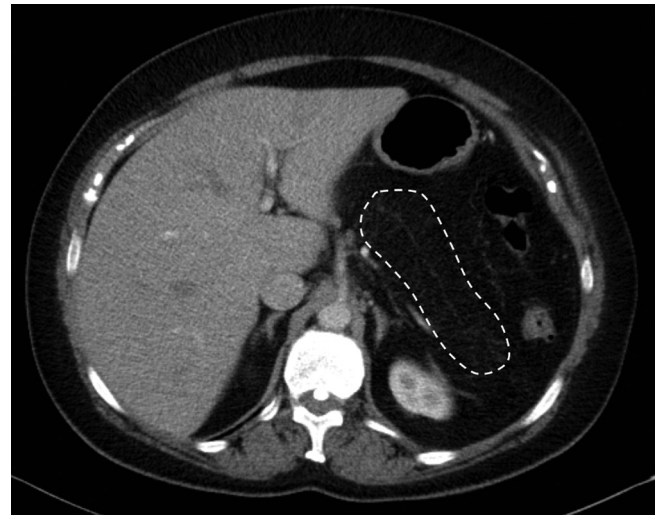
Elastography measures biomechanical tissue response to an applied physical stress. The deep intra-abdominal location of the pancreas precludes the use of transient elastography, but acoustic radiation force impulse (ARFI) can be used to deliver localised stress under standard B-mode ultrasound imaging guidance. Fat deposition is thought to make the liver softer so that stiffness reduces with progressive hepatic steatosis.³⁴ Application in the pancreas has been more limited^{35,36} – studies have hypothesised that reductions in stiffness occur with progressive pancreatic steatosis but results have been conflicting, with one study finding reduced pancreatic stiffness in a group of patients with pancreatic insufficiency in cystic fibrosis³⁷ and another finding no difference between normal pancreatic tissue and NAFLD.³⁶ Nonetheless, this is a growing area and larger-scale studies may yet yield useful applications for NAFLD, albeit limited by the small size of the ARFI region-of-interest (ROI) and difficulties with pancreatic visualisation.

Computed Tomography (CT)

CT is well-suited to imaging the pancreas because of its shorter acquisition time, availability and widespread clinical use. However, the use of ionising radiation and i.v. contrast compromise its use in research, particularly if serial studies are required. Contraindications to i.v. contrast including renal impairment (pertinent in patients with diabetic nephropathy) represent major challenges to use in the assessment of patients with diabetes.

Fatty infiltration of the pancreas is appreciable on CT when there is an increase in interlobular fat (Figure 2), but there are no consensus criteria for the CT diagnosis of pancreatic steatosis. A variety of techniques have been applied in the literature including calculating pancreatic attenuation on unenhanced images using three ROIs placed on the pancreatic head, body and tail. Using this method to derive mean pancreatic attenuation, a threshold of <36 Hounsfield units (HU) has been proposed for the diagnosis of pancreatic steatosis.³⁸ Other studies have used the ratio of pancreatic to splenic attenuation on unenhanced and post-contrast arterial and portal venous phase CTs to demonstrate significant correlations with histological fat fractions.^{27,38} More sophisticated methods of segmentation, including the use of semi-automated techniques to define pancreatic tissue margins, with subsequent histogram analysis with local thresholding have

Figure 2. Complete fatty replacement of the pancreas. Extreme pancreatic steatosis and atrophy – the residual pancreas with presumed borders outlined (dashed white line). The main pancreatic duct is just visible with only minimal lobular tissue.



also been proposed.²⁷ Ectopic fat in the pancreas is not evenly distributed throughout the organ²⁸ and certain patterns of fatty infiltration may be of specific clinical relevance. CT is unable to distinguish between fat in adipocytes and intracellular fat in parenchymal cells so a given ROI may not accurately represent the total organ fat. The pancreatic margin can be poorly defined on CT, particularly in the presence of atrophy, which complicates the placement of ROIs and may result in partial volume effects.

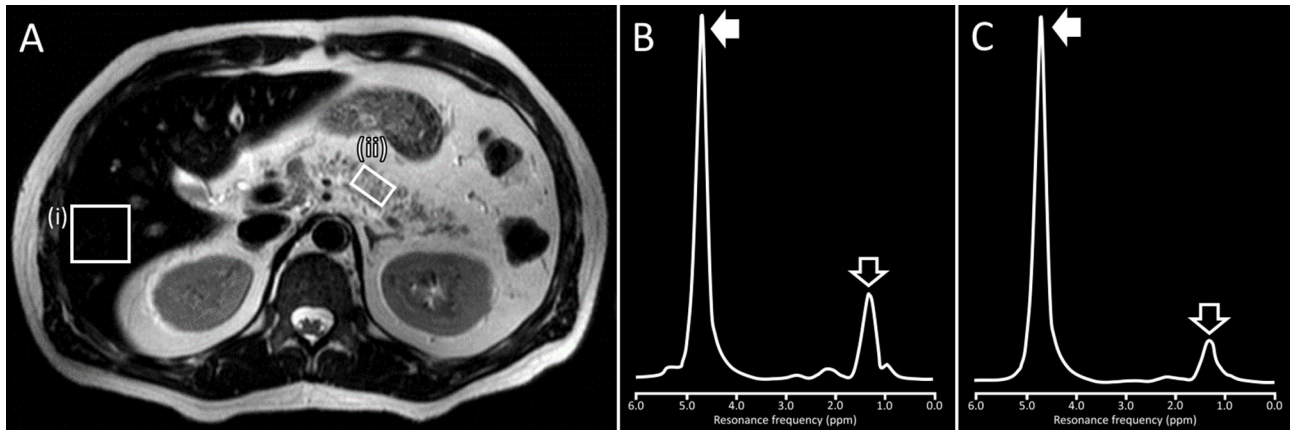
Magnetic Resonance Imaging (MRI)

MR signal from biological tissue arises predominantly from protons within water and fat molecules. Protons within either molecule exist within slightly different chemical environments, giving rise to small differences in their resonance frequencies which can be exploited for quantification.³⁹ MR approaches to fat quantification that have been applied to the pancreas include spectroscopy and imaging methods with early efforts focussing on chemical-shift imaging and evolving into spectral-spatial fat-selective, multipoint Dixon and ultimately proton-density fat fraction (PDFF) techniques.

Magnetic Resonance Spectroscopy (MRS)

MRS is often considered gold-standard for non-invasive pancreatic fat quantification. The technique requires the user to manually position a voxel (usually $2.0 \times 1.0 \times 1.0$ cm, *i.e.* 2.0 cm³) to contain as much pancreatic tissue as possible (avoiding blood vessels and the main pancreatic duct).^{20,25,40–43} MRS acquired using either point-resolved spectroscopy (PRESS) or stimulated echo acquisition mode (STEAM) sequences is used to derive a resonance frequency histogram (spectrum) of the constituent proton signals (Figure 3). Measured raw spectra are then fitted with the expected spectrum and the relative area under spectral peaks of interest (arising from water peaks and detectable peaks for chemical environments of protons within fat) are used to estimate voxel fat fraction.

Figure 3. MRS and the differing spectral complexity of pancreatic fat MRS study planning (a) of the liver (i) and pancreas (ii), with corresponding spectra arising from the liver voxel (b) and pancreatic voxel (c). Note differing voxel sizes and the challenge of ensuring inclusion of purely pancreatic tissue within the MRS voxel (a, ii). The water peak is shown in both spectra (b, c) at 4.7 ppm (solid white arrow). Liver fat spectra (b) have been shown to demonstrate six peaks (at 5.3, 4.2, 2.75, 2.1, 1.3 and 0.9 ppm), while pancreatic fat spectra (c) are dominated by single 1.3 ppm methylene peak (clear white arrow). It is not known if this reflects genuine pancreatic fat content or contamination from extra lobular fat. MRS, magnetic resonance spectroscopy.



Deriving spectra from such a small voxel requires good quality local shimming and multiple averages, thereby extending acquisition time. Susceptibility to respiratory motion and cardiac motion artefact (from adjacent pulsatile arterial vessels) is therefore a major challenge. Voxel contamination with extra pancreatic tissue (usually visceral or peritoneal fat) compromises shim quality and can cause significant alterations in measured spectra. Early studies reported dramatic increases in lipid signal from some measured spectra likely secondary to subject deep breathing.²⁰ Respiratory and cardiac gating have been shown to reduce this challenge but extend acquisition time (as much as 30 min per voxel).⁴¹ Even with respiratory gating, data exclusion rates of as much as 8% due to motion artefact have been reported.⁴³ As imaging protocols are likely to require multivoxel measurements and additional sequences, prolonged acquisition times can conversely result in subject discomfort thereby exacerbating patient motion. Operator expertise in placement of the MRS voxel is also required. The spatial mismatch arising from the time between anatomical imaging used to plan the MRS study and MRS acquisition have also been reported as a source of error.⁴⁴ An issue common to MRS and other imaging-based methods of MR fat quantification arises from the fitting of raw spectra for quantification. Implicit in the fitting process is prior knowledge of where spectral peaks are likely to occur, which is dependent on the chemical environment of intracellular fat and will vary from tissue to tissue. A single broad 1.3 ppm (methylene group) peak has been proposed for the pancreas, but the same peak is also seen in extracellular fat and it is difficult to be certain if measured pancreatic spectra are the result of voxel contamination or arise from intralobular pancreatic tissue itself (Figure 3).⁴⁰ Fitting to incorrect spectra, however has been shown to have significant effects on quantification.^{45,46} Finally, intralobular pancreatic fat content is very low and prone to noise-related errors. Even when diabetic MRS pancreatic fat measurements are increased, this is likely to represent increased fatty infiltration (*i.e.* extralobular fat within the MRS voxel) and age-related loss of beta-cell mass (and

parenchymal volume) rather than impaired beta-cell function arising from a true increase in intralobular fat.⁴⁰

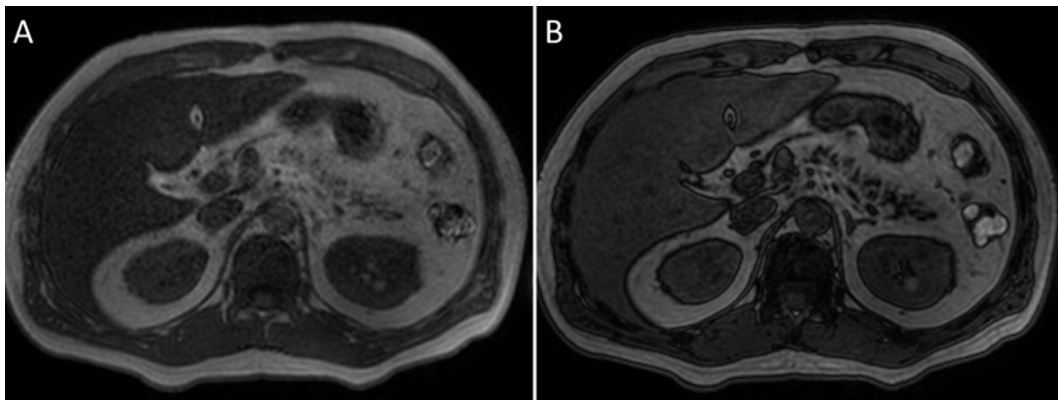
Because of these technical challenges, reported repeatability and reproducibility of pancreatic MRS measurements has been poor, and consistently inferior to that measured in the liver.²⁰ Moreover, reported associations between MRS-derived measurements of pancreatic fat and metabolic factors have been conflicting. MRS studies have confirmed that pancreatic fat is increased in diabetes, obesity^{20,41} and also in the setting of impaired glucose tolerance.²⁵ No association with visceral fat has been reported,^{20,25} and data on the association with beta-cell function has been inconsistent.^{20,43}

Chemical-shift MRI

MR imaging methods have the major advantage of being able to map quantitative data across an entire imaged volume (and not exclusively within a small MRS voxel). More complex hypotheses pertaining to distribution of fat within the pancreas, adjacent abdominal viscera and more distant tissue can then be probed, particularly as MR imaging methods are based on shorter acquisition times. Faster acquisition times are a major strength but also result in limitations to pancreatic fat quantification.

Chemical-shift imaging (CSI) involves acquisition of imaging signal at two or more echo times spaced to match the chemical shift between the main fat and water peaks. Generated "in-phase" and "out-of-phase" images (where fat and water constructively and destructively interfere, respectively), can then be subtracted to estimate fat content.⁴⁷ Qualitative assessment of fat content is feasible, but quantification of tissue fat content is limited by errors arising from background magnetic field (B_0) inhomogeneity, and difficulties with the quantification of very high/low fat fraction measurements.^{39,48} This is a major challenge in a small organ such as the pancreas, where small volume islands of pancreatic parenchymal tissue, surrounded by infiltrating extralobular fat are prone to quantification errors arising from high extralobular

Figure 4. Chemical-shift imaging and pancreatic fat quantification in the presence of fatty infiltration in-phase (a) and out-of-phase (b) CSI in the presence of significant pancreatic fatty infiltration. Note the "india-ink" artefact at fat-water interfaces on out-of-phase images (b), which when combined with in-phase imaging makes quantification in small islands of tissue prone to partial voluming errors. CSI, chemical-shift imaging.



fat content, low pancreatic parenchymal fat and partial voluming (where both extralobular fat and parenchymal fat co-exist within a voxel) (Figure 4).⁴⁰ Studies using CSI have reported correlations between pancreatic and visceral fat, but no association with insulin resistance, BMI, subcutaneous adiposity or other metabolic syndrome features once data was adjusted for the effects of age, gender and visceral adipose tissue.^{49,50}

Several approaches were proposed to overcome the limitations of CSI. Spectral-spatial fat-selective imaging was developed to overcome the challenge of B_0 inhomogeneity, errors arising from noise when quantifying small fat fractions and imaging artefacts that arise at fat-water interfaces (seen at pancreatic tissue boundaries). Using good quality local shimming, spectral-spatial fat-selective imaging applies spectral-selective and spatial-selective excitations within a multislice imaging scheme, to generate fat fraction maps.^{51–53} No correlation between spectral-spatial fat-selective pancreatic and liver fat has been reported,⁵⁴ however negative correlations between pancreatic fat and insulin secretion were observed in patients with impaired glucose tolerance.²⁴

Multipoint Dixon methods were developed to overcome the challenge of B_0 inhomogeneity and ambiguities arising from fat fraction measurements of greater than 50%. Standard CSI relies on signal magnitude acquired from at least two echo times; by imaging at three or more echo times, complex data (including both magnitude and phase images) can be used to map B_0 and correct for inhomogeneities and estimate fat fractions exceeding 50%.⁵⁵ This is important as while pancreatic intralobular fat fractions are low, infiltrating (extra and interlobular) fat is likely to have fat fractions greater than 50%.

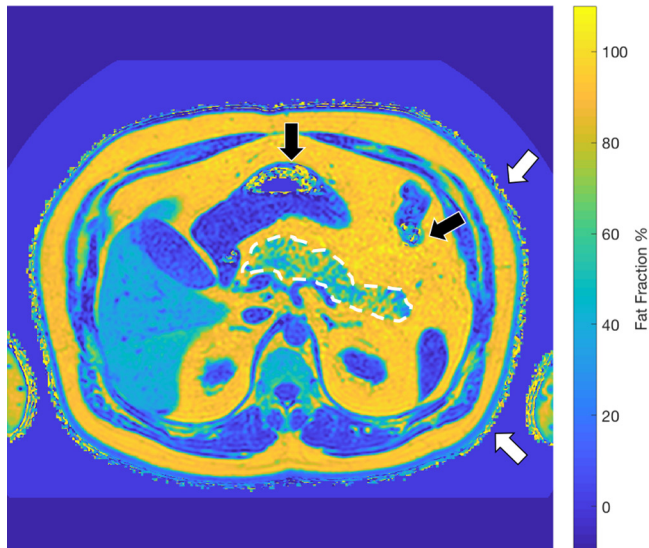
Multipoint Dixon methods have been applied to the pancreas with varying additional modifications for improvement of measurement accuracy. MRS validation studies have demonstrated a tendency to overestimate pancreatic fat fraction,⁴² while histological validation studies have reported wide Bland-Altman limits of agreement (over 16%).⁵⁶

Several studies have reported increased multipoint Dixon pancreatic fat in patients with T2DM,^{40,57,58} with further studies confirming associations between pancreatic fat and age, and weak but significant associations with visceral adiposity and liver fat in adult and paediatric cohorts.^{59,60} Non-uniform increases in multipoint Dixon pancreatic fat fraction in diabetic patients have also been reported, although this may reflect increasing interlobular fatty infiltration/atrophy.⁴⁰ Contrastingly, single-slice whole pancreas (rather than ROI) segmentation demonstrated no significant difference in Type 1 Diabetes Mellitus pancreatic fat relative to normal controls. Large-scale studies however have reported associations with obesity, hypertriglyceridaemia and increased insulin resistance (although these associations were stronger for hepatic fat).^{57,61–63} A small but interesting study demonstrated multipoint Dixon pancreatic fat reductions following an 8-week low calorie diet regime in diabetic patients.⁶⁴

Proton density fat fraction mapping

PDFF mapping addresses limitations of multipoint Dixon quantification, many of which are specifically relevant to pancreatic imaging (Figure 5). T_1 weighting is altered in chronic pancreatic inflammation⁶⁵ and can amplify the relative fat signal. By ensuring the acquisition flip angle is as small as possible, errors introduced by T_1 signal bias can be reduced.⁶⁶ T_2 and T_2^* can both be altered by pancreatic pathology (inflammation and pancreatic iron deposition respectively), furthermore decay of both during the acquisition will also affect fat quantification.⁵⁴ The multiecho time acquisition can be used to measure the amount of T_2 decay, estimate T_2^* and correct for both of these in the fat fraction measurement.⁶⁷ PDFF mapping also accounts for the spectral complexity of fat by modelling fat signal using multipoint fat models, rather than a simple single peak model.^{48,68} Finally, low fat fractions as seen in measurements of intralobular pancreatic fat, suffer from noise bias. Complex data containing positive and negative signal tend to underestimate, whilst magnitude-based methods tend to overestimate, true fat fraction.⁶⁹ Phase constraining/magnitude discrimination methods have been applied to minimise these errors.⁶⁶

Figure 5. Proton density fat fraction imaging images derived from water-only and fat-only are used to generate a parametric fat fraction map across an axial slice. Note low pancreatic intralobular fat fractions (despite fatty infiltration, white-dashed outline). Errors arising from intraluminal (solid black arrows) and peripheral gas (solid white arrows) result in incoherent pixelation.



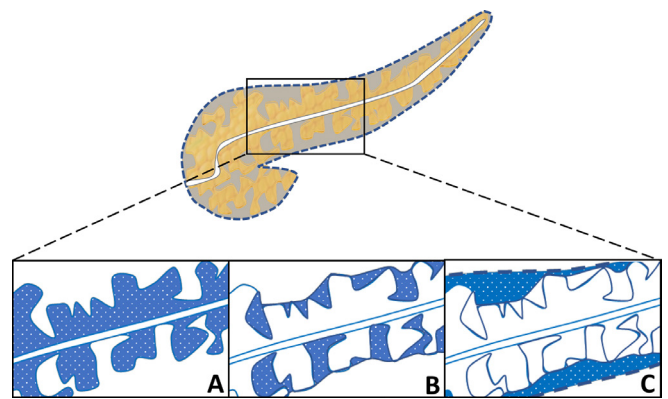
Pancreatic PDFF validation data with MRS has been modest, explained in part by some of the limitations of pancreatic MRS,⁴⁴ and the non-uniform distribution of fat through the pancreas as measured with PDFF.⁷⁰ The association of pancreatic PDFF with diabetes is controversial, with large sample studies reporting increased^{71,72} and unchanged^{70,73} levels of pancreatic fat. Association with insulin resistance has also been reported,⁷⁴ as have modest associations with visceral and subcutaneous adiposity.⁷¹

Challenges and opportunities

Unlike ultrasound and CT, the dependence of MR signal on fat content is a major strength underpinning its use in fat quantification. By avoiding the observer variability of ultrasound and ionising radiation of CT, MRI has the potential to combine spatial, anatomical and quantitative data safely and accurately. The variety of different MRI methods used in the literature is however a challenge, and whilst these catalogue methodological evolution, they also conceal important methodological differences that preclude interstudy comparisons and compromise the pooling of data for meta-analyses.⁹

PDFF MRI currently represents the most evolved method of MR fat quantification but is not without its limitations. The design of PDFF sequences is tailored towards the measurement of hepatic (and not pancreatic) fat and as such there is scope for optimisation that may lead to more robust quantification. The spectral complexity of pancreatic fat has been under investigated, with current presumed *in vivo* spectra prone to contamination from extralobular fat (Figure 3). Surgical specimens for *ex vivo* pancreatic MRS may be a potential approach but are also likely to include significant extralobular fat (especially in the presence of fatty infiltration). Closely linked to this

Figure 6. Pancreatic fat segmentation as the pancreas undergoes both fatty infiltration and atrophy, the significance of fat changes (shaded areas) in the intralobular (a), interlobular (b) and extralobular/peripancreatic (c) fat compartments are unknown. Inconsistencies in the way in which these have been reported/evaluated in the literature are a barrier to pooled meta-analyses and robust segmentation methods for quantifying each of these are an important challenge.



challenge is the lack of reliable reference standard data for validation. Histological sampling is invasive and tends to be derived from surgical specimens (unlike liver biopsies which are more routine and require only minimally invasive image guidance). Measured pancreatic fat fractions are commonly lower than those reported in the liver and are therefore more susceptible to noise. Although the PDFF approach includes methods to minimise noise, it is feasible that a more robust approach is required to deal with the higher levels of noise affecting pancreatic fat measurements.⁶⁹

Approaches to pancreatic segmentation are another area with significant potential for optimisation. Previously discussed studies have classically placed ROIs in the head, body and tail of pancreas, with various specifications to avoid duct, vessel or extra pancreatic fat. Variations in the distribution of fat across the gland have not been consistently described, but this may reflect sampling error. Whole organ segmentation is difficult, as the pancreas can span multiple slices, have ill-defined margins and require significant operator experience/expertise. Recent combinations of manual segmentation with thresholding have shown promising results with improved interobserver variation.⁷⁵ Pancreatic disease however is associated with dramatic morphological changes including fatty infiltration and atrophy. Changes in the distribution of intralobular, interlobular and extralobular pancreatic fat are regularly seen on cross-sectional imaging but remain poorly understood (Figure 6). Improved segmentation methods represent a major tool to address new hypotheses surrounding the distribution of pancreatic fat across these compartments. The development of automated methods for whole organ and multicompartiment segmentation using machine learning methods is a promising area. Whilst to date predominantly focussed on CT,⁷⁶ machine learning has the potential to yield powerful tools for quantitative pancreatic MRI.⁷⁷

Finally, little is known if measured changes in pancreatic fat are due to increases in intracellular fat, parenchymal atrophy or both, or indeed the relationship between and significance of these very different pathophysiological processes in the evolution of metabolic disease and obesity. Recent work on novel subphenotypes within T2DM for example, may yet help to clarify contradictory findings that have emerged from previous pancreatic imaging studies.⁷⁸ Alongside this, the development of better tools for the assessment of pancreatic fat combined with

improvements in our understanding of the microscopic pathophysiology of pancreatic disease will together help to advance the treatment approaches for metabolic disease, diabetes and obesity.

FUNDING

NSS is supported by the National Institute for Health Research (NIHR) University College London Hospitals Biomedical Research Centre. SAT is a NIHR Senior Investigator.

REFERENCES

- Moody A. *Health Survey for England 2015: adult overweight and obesity*. Leeds, UK: NHS Digital; 2016.
- OECD. OECD obesity update. 2017. 2018. Available from: <http://www.oecd.org/health/obesity-update.htm>.
- Britton KA, Fox CS. Ectopic fat depots and cardiovascular disease. *Circulation* 2011; **124**: e837–e841. doi: <https://doi.org/10.1161/CIRCULATIONAHA.111.077602>
- Ogilvie RF. The islands of langerhans in 19 cases of obesity. *J Pathol Bacteriol* 1933; **37**: 473–81. doi: <https://doi.org/10.1002/path.1700370314>
- Martínez J, Johnson CD, Sánchez-Payá J, de Madaria E, Robles-Díaz G, Pérez-Mateo M, et al. Obesity is a definitive risk factor of severity and mortality in acute pancreatitis: an updated meta-analysis. *Pancreatology* 2006; **6**: 206–9. doi: <https://doi.org/10.1159/000092104>
- Lee JS, Kim SH, Jun DW, Han JH, Jang EC, Park JY, et al. Clinical implications of fatty pancreas: correlations between fatty pancreas and metabolic syndrome. *World J Gastroenterol* 2009; **15**: 1869–75. doi: <https://doi.org/10.3748/wjg.15.1869>
- Tariq H, Nayudu S, Akella S, Glandt M, Chilimuri S. Non-alcoholic fatty pancreatic disease: a review of literature. *Gastroenterology Res* 2016; **9**: 87–91. doi: <https://doi.org/10.14740/gr731w>
- Smits MM, van Geenen EJ. The clinical significance of pancreatic steatosis. *Nat Rev Gastroenterol Hepatol* 2011; **8**: 169–77. doi: <https://doi.org/10.1038/nrgastro.2011.4>
- Singh RG, Yoon HD, Wu LM, Lu J, Plank LD, Petrov MS. Ectopic fat accumulation in the pancreas and its clinical relevance: a systematic review, meta-analysis, and meta-regression. *Metabolism* 2017; **69**: 1–13. doi: <https://doi.org/10.1016/j.metabol.2016.12.012>
- Greenberg AS, Obin MS. Obesity and the role of adipose tissue in inflammation and metabolism. *Am J Clin Nutr* 2006; **83**: 461S–5. doi: <https://doi.org/10.1093/ajcn/83.2.461S>
- Juge-Aubry CE, Henrichot E, Meier CA. Adipose tissue: a regulator of inflammation. *Best Pract Res Clin Endocrinol Metab* 2005; **19**: 547–66. doi: <https://doi.org/10.1016/j.beem.2005.07.009>
- Jung UJ, Choi MS. Obesity and its metabolic complications: the role of adipokines and the relationship between obesity, inflammation, insulin resistance, dyslipidemia and nonalcoholic fatty liver disease. *Int J Mol Sci* 2014; **15**: 6184–223. doi: <https://doi.org/10.3390/ijms15046184>
- Mathur A, Marine M, Lu D, Swartz-Basile DA, Saxena R, Zyromski NJ, et al. Nonalcoholic fatty pancreas disease. *HPB* 2007; **9**: 312–8. doi: <https://doi.org/10.1080/13651820701504157>
- Stamm BH. Incidence and diagnostic significance of minor pathologic changes in the adult pancreas at autopsy: a systematic study of 112 autopsies in patients without known pancreatic disease. 2017. Available from: [http://www.humanpathol.com/article/S0046-8177\(84\)80294-4/pdf](http://www.humanpathol.com/article/S0046-8177(84)80294-4/pdf) [accessed 13 Nov2017].
- Lim S, Meigs JB. Ectopic fat and cardiometabolic and vascular risk. *Int J Cardiol* 2013; **169**: 166–76. doi: <https://doi.org/10.1016/j.ijcard.2013.08.077>
- Sepe PS, Ohri A, Sanaka S, Berzin TM, Sekhon S, Bennett G, et al. A prospective evaluation of fatty pancreas by using EUS. *Gastrointest Endosc* 2011; **73**: 987–93. doi: <https://doi.org/10.1016/j.gie.2011.01.015>
- van Geenen EJ, Smits MM, Schreuder TC, van der Peet DL, Bloemena E, Mulder CJ. Nonalcoholic fatty liver disease is related to nonalcoholic fatty pancreas disease. *Pancreas* 2010; **39**: 1185–90. doi: <https://doi.org/10.1097/MPA.0b013e3181f6fce2>
- Pinnick KE, Collins SC, Londos C, Gauquier D, Clark A, Fielding BA. Pancreatic ectopic fat is characterized by adipocyte infiltration and altered lipid composition. *Obesity* 2008; **16**: 522–30. doi: <https://doi.org/10.1038/oby.2007.110>
- Rasouli N, Molavi B, Elbein SC, Kern PA. Ectopic fat accumulation and metabolic syndrome. *Diabetes Obes Metab* 2007; **9**: 1–10. doi: <https://doi.org/10.1111/j.1463-1326.2006.00590.x>
- Tushuizen ME, Bunck MC, Pouwels PJ, Bontemps S, van Waesberghe JH, Schindhelm RK, et al. Pancreatic fat content and beta-cell function in men with and without type 2 diabetes. *Diabetes Care* 2007; **30**: 2916–21. doi: <https://doi.org/10.2337/dc07-0326>
- Wang CY, Ou HY, Chen MF, Chang TC, Chang CJ, H-Y O, Chang C-J. Enigmatic ectopic fat: prevalence of nonalcoholic fatty pancreas disease and its associated factors in a Chinese population. *J Am Heart Assoc* 2014; **3**: e000297. doi: <https://doi.org/10.1161/JAHA.113.000297>
- Yin W, Liao D, Kusunoki M, Xi S, Tsutsumi K, Wang Z, et al. NO-1886 decreases ectopic lipid deposition and protects pancreatic beta cells in diet-induced diabetic swine. *J Endocrinol* 2004; **180**: 399–408. doi: <https://doi.org/10.1677/joe.0.1800399>
- van Raalte DH, van der Zijl NJ, Diamant M. Pancreatic steatosis in humans: cause or marker of lipotoxicity? *Curr Opin Clin Nutr Metab Care* 2010; **13**: 478–85. doi: <https://doi.org/10.1097/MCO.0b013e31832833aa1ef>
- Heni M, Machann J, Staiger H, Schwenzer NF, Peter A, Schick F, et al. Pancreatic fat is negatively associated with insulin secretion in individuals with impaired fasting glucose and/or impaired glucose tolerance: a nuclear magnetic resonance study. *Diabetes Metab Res Rev* 2010; **26**: 200–5. doi: <https://doi.org/10.1002/dmrr.1073>
- van der Zijl NJ, Goossens GH, Moors CC, van Raalte DH, Muskiet MH, Pouwels PJ, et al. Ectopic fat storage in the pancreas, liver, and abdominal fat depots: impact on

- β -cell function in individuals with impaired glucose metabolism. *J Clin Endocrinol Metab* 2011; **96**: 459–67. doi: <https://doi.org/10.1210/jc.2010-1722>
26. Kim MK, Chun HJ, Park JH, Yeo DM, Baek KH, Song KH, et al. The association between ectopic fat in the pancreas and subclinical atherosclerosis in type 2 diabetes. *Diabetes Res Clin Pract* 2014; **106**: 590–6. doi: <https://doi.org/10.1016/j.diabres.2014.09.005>
 27. Lim S, Bae JH, Chun EJ, Kim H, Kim SY, Kim KM, et al. Differences in pancreatic volume, fat content, and fat density measured by multidetector-row computed tomography according to the duration of diabetes. *Acta Diabetol* 2014; **51**: 739–48. doi: <https://doi.org/10.1007/s00592-014-0581-3>
 28. Matsumoto S, Mori H, Miyake H, Takaki H, Maeda T, Yamada Y, et al. Uneven fatty replacement of the pancreas: evaluation with CT. *Radiology* 1995; **194**: 453–. doi: <https://doi.org/10.1148/radiology.194.2.7824726>
 29. Zhou J, Li ML, Zhang DD, Lin HY, Dai XH, Sun XL, et al. The correlation between pancreatic steatosis and metabolic syndrome in a Chinese population. *Pancreatol* 2016; **16**: 578–83. doi: <https://doi.org/10.1016/j.pan.2016.03.008>
 30. Wu WC, Wang CY. Association between Non-Alcoholic Fatty Pancreatic Disease (NAFPD) and the metabolic syndrome: case-control retrospective study. *Cardiovasc Diabetol* 2013; **12**: 77. doi: <https://doi.org/10.1186/1475-2840-12-77>
 31. Lesmana CR, Pakasi LS, Inggriani S, Aidawati ML, Lesmana LA. Prevalence of Non-Alcoholic Fatty Pancreas Disease (NAFPD) and its risk factors among adult medical check-up patients in a private hospital: a large cross sectional study. *BMC Gastroenterol* 2015; **15**: 174. doi: <https://doi.org/10.1186/s12876-015-0404-1>
 32. Della Corte C, Mosca A, Majo F, Lucidi V, Panera N, Giglioni E, et al. Nonalcoholic fatty pancreas disease and nonalcoholic fatty liver disease: more than ectopic fat. *Clin Endocrinol* 2015; **83**: 656–62. doi: <https://doi.org/10.1111/cen.12862>
 33. Choi CW, Kim GH, Kang DH, Kim HW, Kim DU, Heo J, et al. Associated factors for a hyperechogenic pancreas on endoscopic ultrasound. *World J Gastroenterol* 2010; **16**: 4329. doi: <https://doi.org/10.3748/wjg.v16.i34.4329>
 34. Yoneda M, Suzuki K, Kato S, Fujita K, Nozaki Y, Hosono K, et al. Nonalcoholic fatty liver disease: US-based acoustic radiation force impulse elastography. *Radiology* 2010; **256**: 640–7. doi: <https://doi.org/10.1148/radiol.10091662>
 35. Yashima Y, Sasahira N, Isayama H, Kogure H, Ikeda H, Hirano K, et al. Acoustic radiation force impulse elastography for noninvasive assessment of chronic pancreatitis. *J Gastroenterol* 2012; **47**: 427–32. doi: <https://doi.org/10.1007/s00535-011-0491-x>
 36. Goertz RS, Schuderer J, Strobel D, Pfeifer L, Neurath MF, Wildner D. Acoustic radiation force impulse shear wave elastography (ARFI) of acute and chronic pancreatitis and pancreatic tumor. *Eur J Radiol* 2016; **85**: 2211–6. doi: <https://doi.org/10.1016/j.ejrad.2016.10.019>
 37. Friedrich-Rust M, Schlueter N, Smaczny C, Eickmeier O, Rosewich M, Feifel K, et al. Non-invasive measurement of liver and pancreas fibrosis in patients with cystic fibrosis. *J Cyst Fibros* 2013; **12**: 431–9. doi: <https://doi.org/10.1016/j.jcf.2012.12.013>
 38. Kim SY, Kim H, Cho JY, Lim S, Cha K, Lee KH, et al. Quantitative assessment of pancreatic fat by using unenhanced CT: pathologic correlation and clinical implications. *Radiology* 2014; **271**: 104–12. doi: <https://doi.org/10.1148/radiol.13122883>
 39. Bray TJ, Chouhan MD, Punwani S, Bainbridge A, Hall-Craggs MA. Fat fraction mapping using magnetic resonance imaging: insight into pathophysiology. *Br J Radiol* 2017; **20170344**. doi: <https://doi.org/10.1259/bjr.20170344>
 40. Begovatz P, Koliaki C, Weber K, Strassburger K, Nowotny B, Nowotny P, et al. Pancreatic adipose tissue infiltration, parenchymal steatosis and beta cell function in humans. *Diabetologia* 2015; **58**: 1646–55. doi: <https://doi.org/10.1007/s00125-015-3544-5>
 41. Lingvay I, Esser V, Legendre JL, Price AL, Wertz KM, Adams-Huet B, et al. Noninvasive quantification of pancreatic fat in humans. *J Clin Endocrinol Metab* 2009; **94**: 4070–6. doi: <https://doi.org/10.1210/jc.2009-0584>
 42. Livingstone RS, Begovatz P, Kahl S, Nowotny B, Strassburger K, Giani G, et al. Initial clinical application of modified Dixon with flexible echo times: hepatic and pancreatic fat assessments in comparison with (1)H MRS. *MAGMA* 2014; **27**: 397–405. doi: <https://doi.org/10.1007/s10334-013-0421-4>
 43. Szczepaniak LS, Victor RG, Mathur R, Nelson MD, Szczepaniak EW, Tyer N, et al. Pancreatic steatosis and its relationship to β -cell dysfunction in humans: racial and ethnic variations. *Diabetes Care* 2012; **35**: 2377–83. doi: <https://doi.org/10.2337/dc12-0701>
 44. Hu HH, Kim HW, Nayak KS, Goran MI. Comparison of fat-water MRI and single-voxel MRS in the assessment of hepatic and pancreatic fat fractions in humans. *Obesity* 2010; **18**: 841–7. doi: <https://doi.org/10.1038/oby.2009.352>
 45. Reeder SB, Robson PM, Yu H, Shimakawa A, Hines CD, McKenzie CA, et al. Quantification of hepatic steatosis with MRI: the effects of accurate fat spectral modeling. *J Magn Reson Imaging* 2009; **29**: 1332–9. doi: <https://doi.org/10.1002/jmri.21751>
 46. Szczepaniak LS, Dobbins RL, Metzger GJ, Sartoni-D'Ambrosia G, Arbiqwe D, Vongpatanasin W, et al. Myocardial triglycerides and systolic function in humans: in vivo evaluation by localized proton spectroscopy and cardiac imaging. *Magn Reson Med* 2003; **49**: 417–23. doi: <https://doi.org/10.1002/mrm.10372>
 47. Dixon WT. Simple proton spectroscopic imaging. *Radiology* 1984; **153**: 189–94. doi: <https://doi.org/10.1148/radiology.153.1.6089263>
 48. Reeder SB, Cruite I, Hamilton G, Sirlin CB. Quantitative assessment of liver fat with magnetic resonance imaging and spectroscopy. *J Magn Reson Imaging* 2011; **34**: 729–49. doi: <https://doi.org/10.1002/jmri.22580>
 49. Sijens PE, Edens MA, Bakker SJ, Stolk RP. MRI-determined fat content of human liver, pancreas and kidney. *World J Gastroenterol* 2010; **16**: 16. doi: <https://doi.org/10.3748/wjg.v16.i16.1993>
 50. Targher G, Rossi AP, Zamboni GA, Fantin F, Antonioli A, Corzato F, et al. Pancreatic fat accumulation and its relationship with liver fat content and other fat depots in obese individuals. *J Endocrinol Invest* 2012; **35**: 748–53. doi: <https://doi.org/10.3275/8011>
 51. Machann J, Thamer C, Schnoedt B, Stefan N, Haring HU, Claussen CD, et al. Hepatic lipid accumulation in healthy subjects: a comparative study using spectral fat-selective MRI and volume-localized 1H-MR spectroscopy. *Magn Reson Med* 2006; **55**: 913–7. doi: <https://doi.org/10.1002/mrm.20825>
 52. Meyer CH, Pauly JM, Macovski A, Nishimura DG. Simultaneous spatial and spectral selective excitation. *Magn Reson Med* 1990; **15**: 287–304. doi: <https://doi.org/10.1002/mrm.1910150211>
 53. Schick F, Forster J, Machann J, Huppert P, Claussen CD. Highly selective water and fat imaging applying multislice sequences without sensitivity to B1 field inhomogeneities. *Magn Reson Med* 1997; **38**: 269–74. doi: <https://doi.org/10.1002/mrm.1910380216>
 54. Schwenzer NF, Machann J, Martirosian P, Stefan N, Schraml C, Fritsche A, et al. Quantification of pancreatic lipomatosis and liver steatosis by MRI: comparison

- of in/opposed-phase and spectral-spatial excitation techniques. *Invest Radiol* 2008; **43**: 330–7. doi: <https://doi.org/10.1097/RLI.0b013e31816a88c6>
55. Glover GH, Schneider E. Three-point Dixon technique for true water/fat decomposition with B0 inhomogeneity correction. *Magn Reson Med* 1991; **18**: 371–83. doi: <https://doi.org/10.1002/mrm.1910180211>
 56. Yoon JH, Lee JM, Lee KB, Kim SW, Kang MJ, Jang JY, et al. Pancreatic steatosis and fibrosis: quantitative assessment with preoperative multiparametric MR imaging. *Radiology* 2016; **279**: 140–50. doi: <https://doi.org/10.1148/radiol.2015142254>
 57. Dong Z, Luo Y, Cai H, Zhang Z, Peng Z, Jiang M, et al. Noninvasive fat quantification of the liver and pancreas may provide potential biomarkers of impaired glucose tolerance and type 2 diabetes. *Medicine* 2016; **95**: e3858. doi: <https://doi.org/10.1097/MD.0000000000003858>
 58. Raeder H, Haldorsen IS, Erstrand L, Grüner R, Taxt T, Søvik O, et al. Pancreatic lipomatosis is a structural marker in nondiabetic children with mutations in carboxyl-ester lipase. *Diabetes* 2007; **56**: 444–9. doi: <https://doi.org/10.2337/db06-0859>
 59. Lê KA, Ventura EE, Fisher JQ, Davis JN, Weigensberg MJ, Punyanitya M, et al. Ethnic differences in pancreatic fat accumulation and its relationship with other fat depots and inflammatory markers. *Diabetes Care* 2011; **34**: 485–90. doi: <https://doi.org/10.2337/dc10-0760>
 60. Pacifico L, Di Martino M, Anania C, Andreoli GM, Bezzi M, Catalano C, et al. Pancreatic fat and β -cell function in overweight/obese children with nonalcoholic fatty liver disease. *World J Gastroenterol* 2015; **21**: 4688–95. doi: <https://doi.org/10.3748/wjg.v21.i15.4688>
 61. Staaf J, Labmayr V, Paulmichl K, Manell H, Cen J, Ciba I, et al. Pancreatic fat is associated with metabolic syndrome and visceral fat but not beta-cell function or body mass index in pediatric obesity. *Pancreas* 2017; **46**: 358–65. doi: <https://doi.org/10.1097/MPA.0000000000000771>
 62. Wong VW, Wong GL, Yeung DK, Abrigo JM, Kong AP, Chan RS, et al. Fatty pancreas, insulin resistance, and β -cell function: a population study using fat-water magnetic resonance imaging. *Am J Gastroenterol* 2014; **109**: 589–97. doi: <https://doi.org/10.1038/ajg.2014.1>
 63. Yaskolka Meir A, Tene L, Cohen N, Shelef I, Schwarzfuchs D, Gepner Y, et al. Intrahepatic fat, abdominal adipose tissues, and metabolic state: magnetic resonance imaging study. *Diabetes Metab Res Rev* 2017; **33**: e2888. doi: <https://doi.org/10.1002/dmrr.2888>
 64. Lim EL, Hollingsworth KG, Aribisala BS, Chen MJ, Mathers JC, Taylor R. Reversal of type 2 diabetes: normalisation of beta cell function in association with decreased pancreas and liver triacylglycerol. *Diabetologia* 2011; **54**: 2506–14. doi: <https://doi.org/10.1007/s00125-011-2204-7>
 65. Tirkes T, Lin C, Fogel EL, Sherman SS, Wang Q, Sandrasegaran K. T1 mapping for diagnosis of mild chronic pancreatitis. *J Magn Reson Imaging* 2017; **45**: 1171–6.
 66. Liu CY, McKenzie CA, Yu H, Brittain JH, Reeder SB. Fat quantification with IDEAL gradient echo imaging: correction of bias from T₁ and noise. *Magn Reson Med* 2007; **58**: 354–64. doi: <https://doi.org/10.1002/mrm.21301>
 67. O'Regan DP, Callaghan MF, Wylezinska-Arridge M, Fitzpatrick J, Naoumova RP, Hajnal JV, et al. Liver fat content and T2*: simultaneous measurement by using breath-hold multiecho MR imaging at 3.0 T-feasibility. *Radiology* 2008; **247**: 550–7. doi: <https://doi.org/10.1148/radiol.2472070880>
 68. Meisamy S, Hines CD, Hamilton G, Sirlin CB, McKenzie CA, Yu H, et al. Quantification of hepatic steatosis with T1-independent, T2-corrected MR imaging with spectral modeling of fat: blinded comparison with MR spectroscopy. *Radiology* 2011; **258**: 767–75. doi: <https://doi.org/10.1148/radiol.10100708>
 69. Begovatz P, Bierwagen A, Lundbom J, Roden M. Pancreatic triacylglycerol distribution in type 2 diabetes. Reply to Hollingsworth K. G., Al Mrabeh A., Steven S. et al. [letter]. *Diabetologia* 2015; **58**: 2679–81. doi: <https://doi.org/10.1007/s00125-015-3770-x>
 70. Kühn JP, Berthold F, Mayerle J, Völzke H, Reeder SB, Rathmann W, et al. Pancreatic steatosis demonstrated at MR imaging in the general population: clinical relevance. *Radiology* 2015; **276**: 129–36. doi: <https://doi.org/10.1148/radiol.15140446>
 71. Heber SD, Hetterich H, Lorbeer R, Bayerl C, Machann J, Auweter S, et al. Pancreatic fat content by magnetic resonance imaging in subjects with prediabetes, diabetes, and controls from a general population without cardiovascular disease. *PLoS One* 2017; **12**: e0177154. doi: <https://doi.org/10.1371/journal.pone.0177154>
 72. Idilman IS, Tuzun A, Savas B, Elhan AH, Celik A, Idilman R, et al. Quantification of liver, pancreas, kidney, and vertebral body MRI-PDFF in non-alcoholic fatty liver disease. *Abdom Imaging* 2015; **40**: 1512–9. doi: <https://doi.org/10.1007/s00261-015-0385-0>
 73. Patel NS, Peterson MR, Brenner DA, Heba E, Sirlin C, Loomba R. Association between novel MRI-estimated pancreatic fat and liver histology-determined steatosis and fibrosis in non-alcoholic fatty liver disease. *Aliment Pharmacol Ther* 2013; **37**: 630–9. doi: <https://doi.org/10.1111/apt.12237>
 74. Patel NS, Peterson MR, Lin GY, Feldstein A, Schnabl B, Bettencourt R, et al. Insulin resistance increases MRI-estimated pancreatic fat in nonalcoholic fatty Liver disease and normal controls. *Gastroenterol Res Pract* 2013; **2013**: 498296–. doi: <https://doi.org/10.1155/2013/498296>
 75. Al-Mrabeh A, Hollingsworth KG, Steven S, Tiniakos D, Taylor R. Quantification of intrapancreatic fat in type 2 diabetes by MRI. *PLoS One* 2017; **12**: e0174660. doi: <https://doi.org/10.1371/journal.pone.0174660>
 76. p. Roth HR, Farag A, Lu L, Turkbey EB, Summers RM. *Deep convolutional networks for pancreas segmentation in CT imaging*. 8. In: SPIE Medical Imaging. SPIE; 2015.
 77. Gou S, Wu J, Liu F, Lee P, Rapacchi S, Hu P, et al. Feasibility of automated pancreas segmentation based on dynamic MRI. *Br J Radiol* 2014; **87**: 20140248. doi: <https://doi.org/10.1259/bjr.20140248>
 78. Ahlqvist E, Storm P, Käräjämäki A, Martinell M, Dorkhan M, Carlsson A, et al. Novel subgroups of adult-onset diabetes and their association with outcomes: a data-driven cluster analysis of six variables. *Lancet Diabetes Endocrinol* 2018; **6**: 361–9. doi: [https://doi.org/10.1016/S2213-8587\(18\)30051-2](https://doi.org/10.1016/S2213-8587(18)30051-2)